THE JOURNAL OF PHYSICAL CHEMISTRY C

Article

pubs.acs.org/JPCC

Thermal Stability Improvement of *exo*-Tetrahydrodicyclopentadiene by 1,2,3,4-Tetrahydroquinoxaline: Mechanism and Kinetics

Sun Hee Park,[∥,†] Cheong Hoon Kwon,[∥,†] Joongyeon Kim,[†] Jeong Hwan Chun,[†] Wonkeun Chung,[†] Byung-Hee Chun,[†] Jeong Sik Han,[‡] Byung Hun Jeong,[‡] Hogyu Han,*[,§] and Sung Hyun Kim*[,†]

[†]Department of Chemical & Biological Engineering and [§]Department of Chemistry, Korea University, Seoul 136-701, Korea

[‡]Agency for Defense Development, 111 Sunam-dong, Yuseong-gu, Daejeon 305-152, Korea

Supporting Information

ABSTRACT: We investigated the thermal stability of *exo*-tetrahydrodicyclopentadiene (*exo*-THDCP, $C_{10}H_{16}$) in the absence and presence of three additives, 3,4-dihydro-2H-1,4-benzoxazine (Benzox), 1,2,3,4-tetrahydroquinoline (THQ), and 1,2,3,4-tetrahydroquinoxaline (THQox), which act as hydrogen donors (H donors). Conversion of *exo*-THDCP was slowed in the presence of the H donor. The order of the H-donor effects on the decrease in the conversion of *exo*-THDCP was Benzox ≪ THQ < THQox. The H-donor-induced decrease in the conversion of *exo*-THDCP was smaller at higher temperature. In addition, the H-donor-induced decrease in the rate of $<C_{10}$ product formation was smaller than that of $\geq C_{10}$. We proposed the mechanism for the thermal decomposition of *exo*-THDCP in the presence of the H donor. The proposed mechanism explains the unusual thermal decomposition kinetics of *exo*-THDCP and H donors: (i) *exo*-THDCP does not follow first-order kinetics and (ii) THQ and THQox show the S-shaped concentration−time curves. We also proposed the mechanism for H donations by Benzox, THQ, and THQox. The proposed mechanism elucidates that THQox performs faster H donation than THQ and has higher thermal stability than Benzox, which accounts for the more effective thermal stability improvement of *exo*-THDCP by THQox compared to THQ and Benzox.

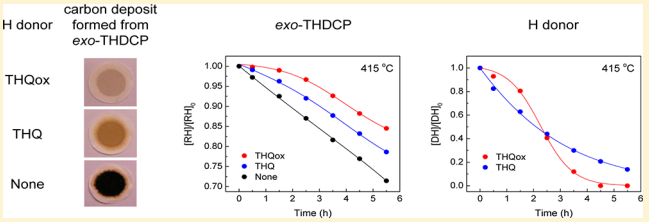

1. INTRODUCTION

Fuel is subjected to temperatures above 370 °C in aircraft flying at speeds greater than Mach 4.[1,2] Since fuel degradation and carbon deposit formation thereupon at this temperature can cause problems for the engine and subsystem, the thermal stability of fuel is important for their proper functioning.

exo-Tetrahydrodicyclopentadiene (*exo*-THDCP, $C_{10}H_{16}$, *exo*-tricyclo[5.2.1.0^{2,6}]decane) is a synthetic liquid fuel with a bridged ring structure.[3−26] *exo*-THDCP has attracted significant attention as a high energetic material (HEM), which is suitable for use in volume-limited aircraft.[3,4,7−9]

A promising approach to enhance the thermal stability of fuel is the use of thermal stabilizers.[27−43] Many previous studies on thermal stabilizers have focused on hydrogen donors (H donors), such as 1,2,3,4-tetrahydroquinoline (THQ), benzyl alcohol (BnOH), and tetralin (THN). H donors terminate the propagation of radicals produced upon thermal decomposition of fuel. H donors are then converted to thermally and chemically stable compounds.[30] Among H donors, THQ has been known to be the most effective thermal stabilizer.[27,30,31,38,40−43] THQ enhances the thermal stability of kerosene-based fuels (Jet A-1, JP-8, RP-1, and RP-2), model hydrocarbon fuels (*n*-dodecane and methylcyclohexane), and biodiesel fuels.

Recently, we reported that THQ also improved the thermal stability of *exo*-THDCP.[25] We proposed the mechanism for the thermal decomposition of *exo*-THDCP, which explains the H-donor-induced thermal stability improvement of *exo*-THDCP. The proposed mechanism suggests that the thermal stability of *exo*-THDCP can be further improved by effective additives capable of performing faster H donation than THQ. However, such effective additives have not been sought yet.

Here, we report the study on the thermal stability of *exo*-THDCP in the absence and presence of 3,4-dihydro-2H-1,4-benzoxazine (Benzox), THQ, and 1,2,3,4-tetrahydroquinoxaline (THQox) (Figure 1). The thermal stability of *exo*-THDCP was improved by the H donors. The order of the H-donor effects on the thermal stability improvement of *exo*-THDCP was Benzox ≪ THQ < THQox. We proposed the mechanism for the thermal decomposition of *exo*-THDCP in the presence

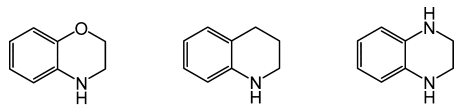

Figure 1. H donors studied for their effects on the thermal stability of *exo*-THDCP.

Received: November 17, 2012
Revised: February 1, 2013
Published: February 5, 2013

 © 2013 American Chemical Society

of the H donor, which explains their unusual thermal decomposition kinetics. We also proposed the mechanism for H donations by Benzox, THQ, and THQox, which elucidates their distinct H-donation kinetics and thermal stability and thereby accounts for the more effective thermal stability improvement of *exo*-THDCP by THQox compared to THQ and Benzox.

2. EXPERIMENTAL SECTION

2.1. Materials and Experimental Methods. Benzox was purchased from Combi−Blocks (San Diego, CA). THQ and THQox were purchased from Sigma−Aldrich.

Thermal decomposition of *exo*-THDCP (100 mL) was carried out in a batch reactor (160 mL) as reported previously.[25] A quartz flask was inserted inside the stainless steel reactor and a quartz plate was placed on the inside of the stainless steel reactor cover. Quartz was used to block any possible catalytic role of stainless steel or other metals.

Hydrocarbon compounds and the hydrogen molecule were analyzed on gas chromatography−mass spectrometry (GC−MS, Agilent 7890A, 5975C), GC−flame ionization detection (GC−FID, Agilent 7890A), and GC−thermal conductivity detection (GC−TCD, Agilent 7890A) systems as reported previously.[25]

The amount of carbon deposit formed in the fuel and on the flask wall upon thermal decomposition of *exo*-THDCP was measured by weighing solid deposit, which was collected on the filter paper and left on the flask wall, respectively, after the fuel was filtered off.

Conversion of *exo*-THDCP and the composition of the product were measured as reported previously.[25] Conversion of *exo*-THDCP is defined as

$$\text{conversion of } \textit{exo}\text{-THDCP}(\%) = \frac{[\mathrm{RH}]_0 - [\mathrm{RH}]}{[\mathrm{RH}]_0} \times 100$$

where $[\mathrm{RH}]_0$ and $[\mathrm{RH}]$ are the concentrations (wt %) of *exo*-THDCP at the initial and indicated times, respectively. $[\mathrm{RH}]$ was determined by GC analysis as described above. The composition of the product is defined as the ratio (wt %/wt %) of C_n to all compounds, where C_n indicates all compounds with n number of carbons, unless otherwise noted.

2.2. Kinetic Analysis. We carried out the kinetic analysis of the thermal decomposition of *exo*-THDCP in the presence of the H donor. Our proposed mechanism for the thermal decomposition of *exo*-THDCP (RH) in the presence of a H donor (DH) is as follows:

$$\mathrm{RH} \xrightarrow{k_1} \mathrm{R}\cdot + \mathrm{H}\cdot \quad (1)$$

$$\mathrm{R}\cdot \xrightarrow{k_2} \mathrm{R}'\cdot \quad (2)$$

$$\mathrm{DH} \xrightarrow{k_3} \mathrm{D} + \mathrm{H}\cdot \quad (3)$$

$$\mathrm{R}\cdot + \mathrm{DH} \xrightarrow{k_4} \mathrm{RH} + \mathrm{D} \quad (4)$$

$$\mathrm{H}\cdot + \mathrm{DH} \xrightarrow{k_5} \mathrm{H_2} + \mathrm{D} \quad (5)$$

$$\mathrm{R}'\cdot + \mathrm{DH} \xrightarrow{k_6} \mathrm{R}'\mathrm{H} + \mathrm{D} \quad (6)$$

Radical formation steps 1−3 involve the H abstraction of RH, radical rearrangement (or fragmentation), and the H abstraction of DH, respectively, whereas radical termination steps 4−6 involve H addition.

Rate equations for the formations of $[\mathrm{RH}]$, $[\mathrm{DH}]$, $[\mathrm{R}\cdot]$, $[\mathrm{H}\cdot]$, and $[\mathrm{R}'\cdot]$ are as follows:

$$\frac{d[\mathrm{RH}]}{dt} = -k_1[\mathrm{RH}] + k_4[\mathrm{R}\cdot][\mathrm{DH}] \quad (7)$$

$$\frac{d[\mathrm{DH}]}{dt} = -(k_3 + k_4[\mathrm{R}\cdot] + k_5[\mathrm{H}\cdot] + k_6[\mathrm{R}'\cdot])[\mathrm{DH}] \quad (8)$$

$$\frac{d[\mathrm{R}\cdot]}{dt} = k_1[\mathrm{RH}] - k_2[\mathrm{R}\cdot] - k_4[\mathrm{R}\cdot][\mathrm{DH}] \quad (9)$$

$$\frac{d[\mathrm{H}\cdot]}{dt} = k_1[\mathrm{RH}] + k_3[\mathrm{DH}] - k_5[\mathrm{H}\cdot][\mathrm{DH}] \quad (10)$$

$$\frac{d[\mathrm{R}'\cdot]}{dt} = k_2[\mathrm{R}\cdot] - k_6[\mathrm{R}'\cdot][\mathrm{DH}] \quad (11)$$

We assume a steady-state approximation for all the radicals $[\mathrm{R}\cdot]$, $[\mathrm{H}\cdot]$, and $[\mathrm{R}'\cdot]$:

$$\frac{d[\mathrm{R}\cdot]}{dt} = \frac{d[\mathrm{H}\cdot]}{dt} = \frac{d[\mathrm{R}'\cdot]}{dt} \approx 0 \quad (12)$$

Combining eqs 7−12, we obtain differential rate eqs 13 and 14 for the formations of $[\mathrm{RH}]$ and $[\mathrm{DH}]$:

$$\frac{d[\mathrm{RH}]}{dt} = -k_1[\mathrm{RH}] + \frac{k_1k_4}{k_2'}[\mathrm{RH}][\mathrm{DH}] \quad (13)$$

$$\frac{d[\mathrm{DH}]}{dt} = -2k_1[\mathrm{RH}] - 2k_3[\mathrm{DH}] \quad (14)$$

where $k_2' = k_2 + k_4[\mathrm{DH}]$, which is assumed to be nearly constant.

From the first-order differential eqs 13 and 14, we obtain the second-order differential eqs 15 and 16:

$$\frac{d^2[\mathrm{RH}]}{dt^2} + \left(2k_3 - \frac{1}{[\mathrm{RH}]}\frac{d[\mathrm{RH}]}{dt}\right)\frac{d[\mathrm{RH}]}{dt} = F([\mathrm{RH}]) \quad (15)$$

$$\frac{d^2[\mathrm{DH}]}{dt^2} + \left(k_1 + 2k_3 - \frac{k_1k_4}{k_2'}[\mathrm{DH}]\right)\frac{d[\mathrm{DH}]}{dt} = G([\mathrm{DH}]) \quad (16)$$

$$\text{where} \quad F([\mathrm{RH}]) = -2k_1k_3[\mathrm{RH}] - 2\frac{k_1^2k_4}{k_2'}[\mathrm{RH}]^2$$

$$G([\mathrm{DH}]) = -2k_1k_3[\mathrm{DH}] + 2\frac{k_1k_3k_4}{k_2'}[\mathrm{DH}]^2$$

We assume $F([\mathrm{RH}]) \neq 0$ and $G([\mathrm{DH}]) = 0$. Solving the differential rate eqs 15 and 16 and then normalizing the integrated rate equations thus obtained for $[\mathrm{RH}]$ and $[\mathrm{DH}]$ over their initial concentrations, we obtain the final expressions of $[\mathrm{RH}]/[\mathrm{RH}]_0$ and $[\mathrm{DH}]/[\mathrm{DH}]_0$ in terms of the reaction time t as follows:

$$\frac{[\mathrm{RH}]}{[\mathrm{RH}]_0} \approx e^{-kt}\frac{A^2(k_1(A-1) - (k-k_1)e^{-kt})}{(A-1+e^{-kt})^2(k_1(A-1) - (k-k_1))} \quad (17)$$

$$\frac{[\mathrm{DH}]}{[\mathrm{DH}]_0} \approx \frac{Ae^{-kt}}{A-1+e^{-kt}} \quad (18)$$

dx.doi.org/10.1021/jp3113599 | J. Phys. Chem. C 2013, 117, 7399−7407

$$\text{where} \quad A = \frac{2kk_2'}{k_1k_4}\frac{1}{[\mathrm{DH}]_0} \quad \text{and} \quad k = k_1 + 2k_3$$

By using the Nonlinear Curve Fit method in the OriginPro (ver. 8.5.1) software, experimental data were fitted to eqs 17 and 18 with regression parameters k_1, k, and A, whereupon k_3 and k_4/k_2' were obtained.

2.3. Molecular Mechanics Calculation. The geometry optimized structures and energies of H donors and their intermediates and products were calculated using the molecular mechanics (MM3) method in the MOPAC program (Fujitsu CAChe 7.7).[44−46] The geometry optimized structures thus obtained were then employed to calculate the energy changes for bond breaking and forming processes using the MM3 method. Such energy changes were used to determine the possible reaction pathways for H donation. In Benzox, for example, we first examined the energy change for three possible pathways in the H donation from N1−H (−18.7 kJ/mol), C2−H (−4.0 kJ/mol), and C3−H (−6.9 kJ/mol) of reactant **1a** to form intermediate $\mathbf{I}_{\mathbf{1a}}$. Considering that a reaction progresses toward intermediates and products when the energy release is maximized for such progresses, we then predicted that the N1−H bond cleavage would most likely occur in the first step.

3. RESULTS AND DISCUSSION

3.1. H-Donor Effects on the Conversion of *exo*-THDCP. Conversions of *exo*-THDCP in the absence and presence of H donors (0.5 wt %) at 395 and 415 °C are shown in Figure 2. Conversions of *exo*-THDCP in the absence of the H donor were 8.7% and 28.9% at 395 and 415 °C for 5.5 h, respectively (Figure 2a and b, solid black circles and left *y* axis). Thus, conversion of *exo*-THDCP was faster at the higher temperature. Conversions of *exo*-THDCP in the presence of Benzox, THQ, and THQox were 7.4%, 4.0%, and 0.6% at 395 °C for 5.5 h and 29.0%, 21.8%, and 15.6% at 415 °C for 5.5 h, respectively (Figure 2a and b, solid green, blue, and red circles and left *y* axis). Thus, conversion of *exo*-THDCP was slowed in the presence of the H donor. The order of the H-donor effects on the decrease in the conversion of *exo*-THDCP was Benzox ≪ THQ < THQox. Conversions of *exo*-THDCP in the presence of Benzox, THQ, and THQox compared to their absence decreased by 1.3%, 4.7%, and 8.1% at 395 °C for 5.5 h and −0.1%, 7.1%, and 13.3% at 415 °C for 5.5 h, respectively. Actually, conversion of *exo*-THDCP was hardly slowed in the presence of Benzox at 415 °C. Thus, the H-donor-induced decrease in the conversion of *exo*-THDCP was smaller at the higher temperature.

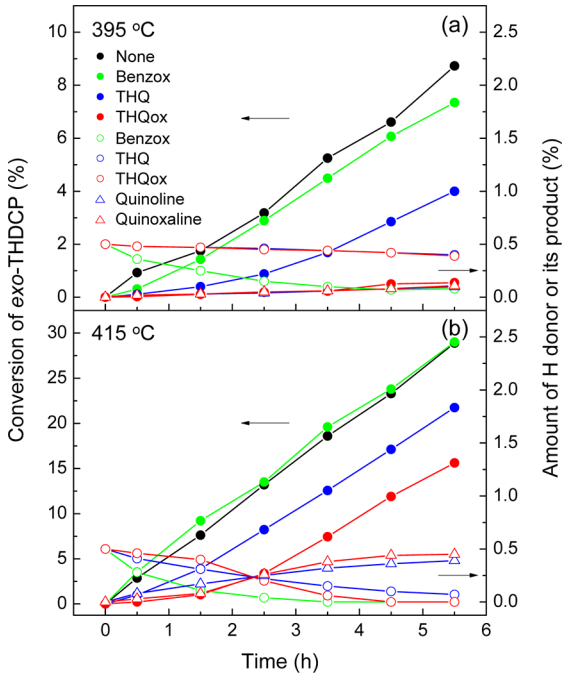

Figure 2. Conversions of *exo*-THDCP in the absence and presence of H donors (0.5 wt %) at 395 and 415 °C. Conversion of *exo*-THDCP and the amounts of H donor and its product are indicated by solid circles (left *y* axis) and open circles and triangles (right *y* axis), respectively.

At 395 °C, the average consumption (formation) rates of Benzox, THQ, and THQox (quinoline and quinoxaline) were almost constant (0.070, 0.017, and 0.018%/h (0.017 and 0.018%/h)) during the entire reaction (Figure 2a, open circles (triangles) and right *y* axis). Note that conversion of *exo*-THDCP was slower in the presence of THQox compared to THQ and Benzox during the entire reaction at 395 °C (Figure 2a, solid red, blue, and green circles and left *y* axis). Thus, conversion of *exo*-THDCP was more effectively slowed by THQox compared to THQ and Benzox despite the nearly identical or slower consumption rate of THQox. It seems that THQox performs faster H donation than THQ at 395 °C, thereby terminating more effectively the propagation of radicals produced upon thermal decomposition of *exo*-THDCP. After H donations, THQ and THQox were converted into quinoline and quinoxaline, respectively (Figure 2a, open circles and triangles and right *y* axis). However, Benzox was converted to undetectable products. It seems that Benzox undergoes thermal decomposition without significantly affecting the conversion of *exo*-THDCP at 395 °C. Taken together, THQox appears to perform faster H donation than THQ and has higher thermal stability than Benzox at 395 °C.

At 415 °C, the average consumption (formation) rates of Benzox and THQ (quinoline) were almost constant (0.125 and 0.072%/h (0.065%/h)) during the entire reaction, whereas that of THQox (quinoxaline) varied with the reaction time (0.049, 0.171, and 0.060%/h (0.044, 0.156, and 0.055%/h) for early, middle, and late ∼2 h) (Figure 2b, open circles (triangles) and right *y* axis). Note that conversion of *exo*-THDCP was slower in the presence of THQox compared to THQ and Benzox during the entire reaction at 415 °C (Figure 2b, solid red, blue, and green circles and left *y* axis). Thus, conversion of *exo*-THDCP was more effectively slowed by THQox compared to THQ and Benzox at the slower and faster consumption rates of *exo*-THDCP in the early and middle stages of the reaction. It seems that THQox performs faster H donation than THQ even at 415 °C. In the early stage of the reaction, where there are small amounts of radicals formed mainly from *exo*-THDCP, the small propagation of radicals can be terminated more effectively by additives capable of performing faster H donation without high additive consumption. In the middle stage of the reaction, where there are large amounts of radicals, their massive propagation cannot be terminated effectively even by such additives without high additive consumption. Conversion of *exo*-THDCP was no longer slowed by Benzox despite its fast consumption rate at 415 °C. After H donations, THQ and THQox were converted into quinoline and quinoxaline, respectively (Figure 2b, open circles and triangles and right *y* axis). However, Benzox was converted to undetectable

dx.doi.org/10.1021/jp3113599 | J. Phys. Chem. C 2013, 117, 7399−7407

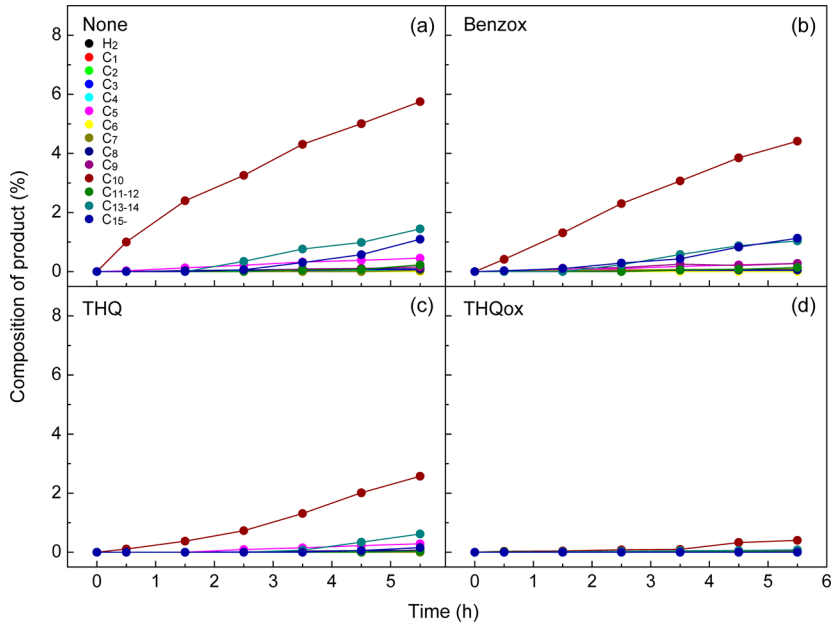

Figure 3. Compositions of products formed upon thermal decomposition of *exo*-THDCP in the absence and presence of H donors (0.5 wt %) at 395 °C. Products are classified by the number of carbons. Note that the plot for C_{10} shown here was obtained with the ratio of C_{10} minus observed (not initial) *exo*-THDCP to all compounds. For small compositions of products, see Figure S1 of the Supporting Information.

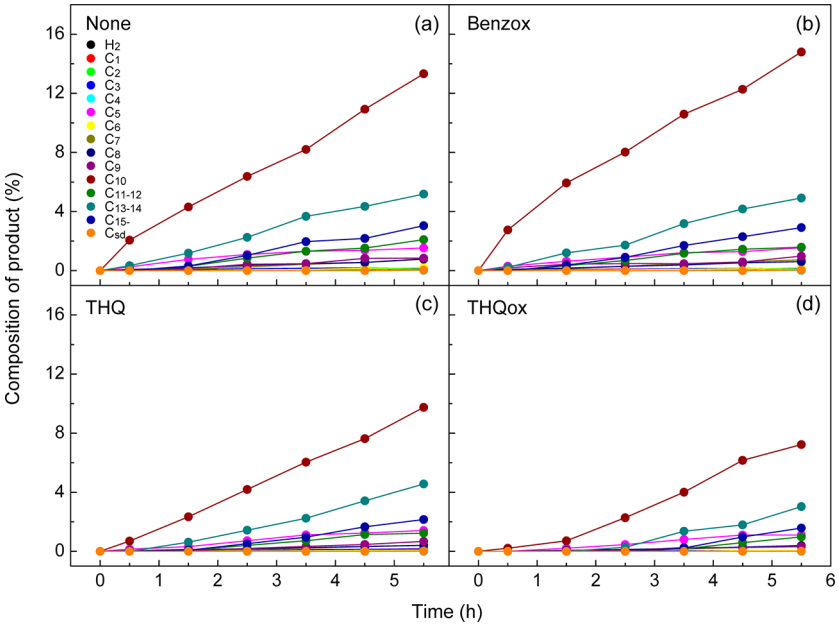

Figure 4. Compositions of products formed upon thermal decomposition of *exo*-THDCP in the absence and presence of H donors (0.5 wt %) at 415 °C. Products are classified by the number of carbons. Note that the plot for C_{10} shown here was obtained with the ratio of C_{10} minus observed (not initial) *exo*-THDCP to all compounds. For small compositions of products, see Figure S2 of the Supporting Information.

products. It seems that Benzox undergoes thermal decomposition without affecting the conversion of *exo*-THDCP any more at 415 °C. Taken together, THQox appears to perform fast H donation without its significant thermal decomposition even at 415 °C.

3.2. H-Donor Effects on Compositions of Products Formed from *exo*-THDCP. Compositions of products formed from *exo*-THDCP in the absence and presence of H donors (0.5 wt %) at 395 °C are shown in Figure 3. Most of the products were C_{10} compounds regardless of whether H donors were present or not. C_{10} compounds formed from *exo*-THDCP were its primary decomposition products as reported previously.[25] The secondary decomposition products, which are formed via fragmentation or recombination and thus obtained mostly as H_2, $<C_{10}$, and $>C_{10}$ compounds, were hardly formed in the presence of THQ and THQox at 395 °C.

Compositions of products formed from *exo*-THDCP in the absence and presence of H donors (0.5 wt %) at 415 °C are shown in Figure 4. Most of the products were the primary decomposition products (C_{10} compounds) at 415 °C regardless of whether H donors were present or not, although their ratio to all compounds (products) increased (decreased) as

dx.doi.org/10.1021/jp3113599 | J. Phys. Chem. C 2013, 117, 7399−7407

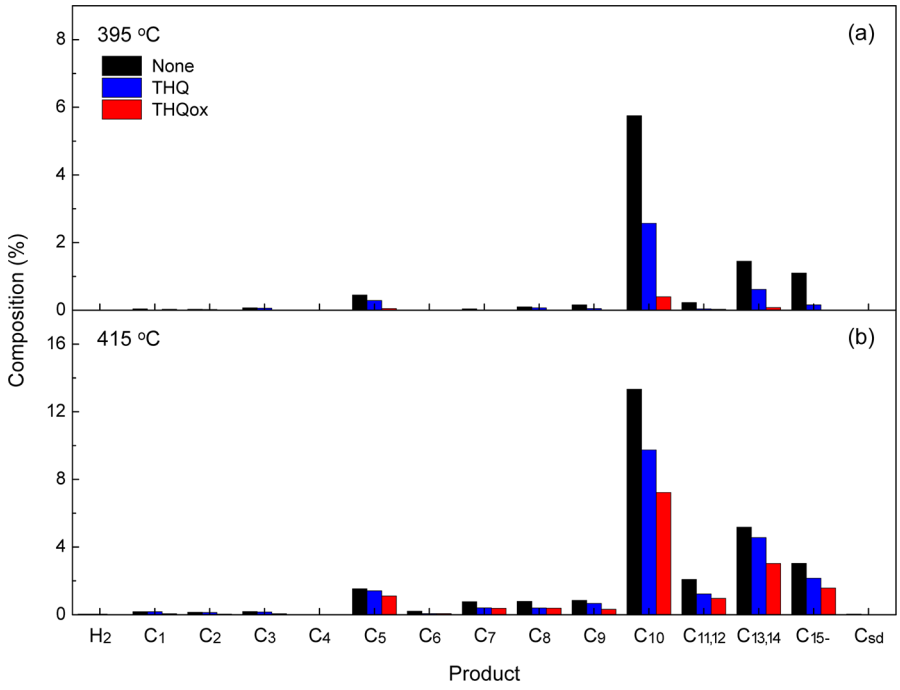

Figure 5. Comparison of product compositions obtained upon thermal decomposition of *exo*-THDCP in the absence and presence of THQ and THQox (0.5 wt %) at 395 and 415 °C for 5.5 h. See also Figures 3 and 4 and Table 1.

Table 1. Comparison of Product Compositions Obtained upon Thermal Decomposition of *exo*-THDCP in the Absence and Presence of THQ and THQox (0.5 wt %) at 395 and 415 °C for 5.5 h[a]

	395 °C						415 °C					
	yield, Y (wt %)						yield, Y (wt %)					
product	none	THQ	THQox	Δ_{THQ}	Δ_{THQox}	$\Delta_{THQox-THQ}$	none	THQ	THQox	Δ_{THQ}	Δ_{THQox}	$\Delta_{THQox-THQ}$
H_2	0.00	0.00	0.00	0.00	0.00	0.00	0.04	0.04	0.01	0.00	−0.03	−0.03
C_{1-4}	0.14	0.09	0.05	−0.05	−0.09	−0.04	0.52	0.47	0.16	−0.05	−0.36	−0.31
C_5	0.45	0.29	0.05	−0.16	−0.40	−0.24	1.54	1.41	1.11	−0.13	−0.43	−0.30
C_{6-9}	0.30	0.12	0.00	−0.18	−0.30	−0.12	2.62	1.55	1.16	−1.07	−1.46	−0.39
C_{10}	5.75	2.57	0.40	−3.18	−5.35	−2.17	13.3	9.75	7.23	−3.55	−6.07	−2.52
C_{11-14}	1.68	0.66	0.11	−1.02	−1.57	−0.55	7.27	5.79	4.00	−1.48	−3.27	−1.79
C_{15-}	1.10	0.16	0.00	−0.94	−1.10	−0.16	3.04	2.16	1.58	−0.88	−1.46	−0.58
C_{sd}	0.000	0.000	0.000	0.000	0.000	0.000	0.041	0.022	0.009	−0.019	−0.032	−0.013

[a]See also Figure 5. Note that the composition of the product is also referred to as the yield. $\Delta_{THQ} = Y_{THQ} - Y_{none}$; $\Delta_{THQox} = Y_{THQox} - Y_{none}$; $\Delta_{THQox-THQ} = Y_{THQox} - Y_{THQ}$.

compared to that at 395 °C. However, the secondary decomposition products (H_2, $<C_{10}$, and $>C_{10}$ compounds) were formed in larger amount at 415 °C than at 395 °C even in the presence of THQ and THQox. Note that C_{sd} solid deposit was produced at 415 °C. The ratio of C_{sd} to all compounds in the absence and presence of Benzox, THQ, and THQox at 415 °C for 5.5 h was 0.041%, 0.040%, 0.022%, and 0.009%, respectively.

Comparison of product compositions obtained from *exo*-THDCP in the absence and presence of THQ and THQox (0.5 wt %) at 395 and 415 °C for 5.5 h are shown in Figure 5 and Table 1 and Figure S3 and Table S1 of the Supporting Information. The ratios of H_2, C_{1-4}, C_5, C_{6-9}, C_{10}, C_{11-14}, C_{15-}, and C_{sd} to all compounds at 395 °C (415 °C) for 5.5 h at 0.5% THQ and THQox compared to 0.0% H donor, where conversions of *exo*-THDCP were 4.0%, 0.6%, and 8.7% (21.8%, 15.6%, and 28.9%), decreased by the absolute Δ_{THQ} and Δ_{THQox} values for H_2 and C_n in Table 1. Thus, their ratios to all products in the presence of THQ and THQox compared to their absence increased or decreased by the absolute Δ_{THQ} and Δ_{THQox} values for H_2 and C_n in Table S1 of the Supporting Information. Accordingly, the ratios of $<C_{10}$ ($\geq C_{10}$) to all products in the presence of THQ and THQox compared to their absence increased or decreased by the sum of the absolute Δ_{THQ} or Δ_{THQox} values for H_2, C_{1-4}, C_5, and C_{6-9} (C_{10}, C_{11-14}, C_{15-}, and C_{sd}) in Table S1 of the Supporting Information. These Δ_{THQ} and Δ_{THQox} values for $<C_{10}$ ($\geq C_{10}$) were 3.5% and 7.0% (−3.4% and −6.9%) at 395 °C. Thus, the H-donor-induced decrease in the rate of $<C_{10}$ product formation was smaller than that of $\geq C_{10}$. The H-donor-induced decrease in the rate of $<C_{10}$ ($\geq C_{10}$) product formation was smaller (higher) in the presence of THQox compared to THQ.

The amounts of carbon deposit formed upon thermal decomposition of *exo*-THDCP in the absence and presence of H donors (0.5 wt %) at 415 °C for 5.5 h are shown in Figure 6. The amounts of carbon deposits in the absence and presence of Benzox, THQ, and THQox were 37.0, 36.7, 20.3, and 8.3 mg in 100 mL of *exo*-THDCP used, respectively. Thus, the order of

dx.doi.org/10.1021/jp3113599 | J. Phys. Chem. C 2013, 117, 7399−7407

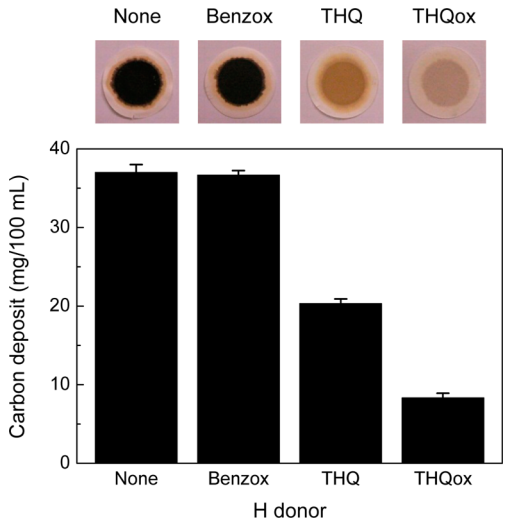

Figure 6. Amounts of carbon deposit formed upon thermal decomposition of *exo*-THDCP in the absence and presence of H donors (0.5 wt %) at 415 °C for 5.5 h.

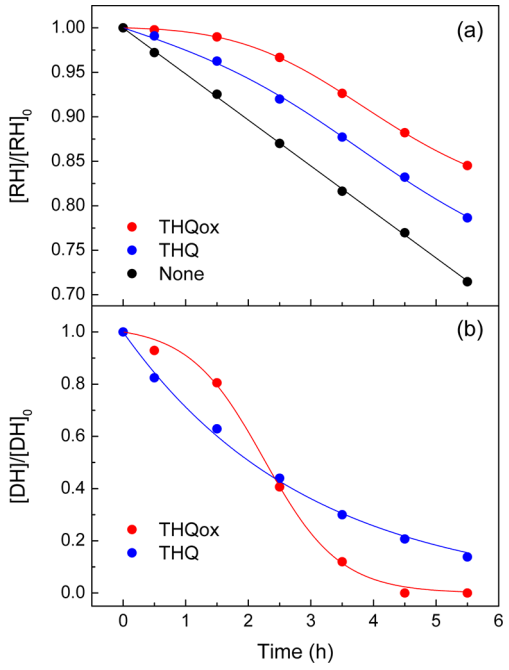

Figure 7. Kinetic analyses of the thermal decomposition of *exo*-THDCP in the absence and presence of THQ and THQox (0.5 wt %) at 415 °C. Experimental data (red and blue circles) for *exo*-THDCP (a) and H donors (b) were fitted to eqs 17 and 18 (curves) in Section 2.2, respectively. Experimental data (black circles) for *exo*-THDCP in (a) were fitted to $[RH]/[RH]_0 \approx 1 - k_1 t$ (line), which is derived from $\ln [RH]/[RH]_0 = -k_1 t$ when $1 - [RH]/[RH]_0 \ll 1$. Note that $\ln [RH]/[RH]_0 = -k_1 t$ is the integrated rate equation for first-order kinetics. For the fitting kinetic parameters, see Table 2.

the H-donor-induced effects on the decrease in carbon deposit formation is Benzox < THQ < THQox. Note the same order of the H-donor-induced effects on the decrease in the conversion of *exo*-THDCP. Accordingly, the amount of carbon deposit decreased as conversion of *exo*-THDCP was decreased by H donors.

We can summarize the key experimental results on compositions of products formed from *exo*-THDCP in the absence and presence of H donors as follows.

(i) The H-donor-induced decrease in the rate of $<C_{10}$ product formation was smaller than that of $\geq C_{10}$.
(ii) The H-donor-induced decrease in the rate of $<C_{10}$ ($\geq C_{10}$) product formation was smaller (higher) in the presence of a more effective H donor.

Our previously proposed mechanism for the thermal decomposition of *exo*-THDCP explains the experimental results (i) and (ii) (see Figure 11 in ref 25). According to the mechanism, *exo*-THDCP is converted to C_{10} radical intermediates via C−C cleavage or H abstraction. They are then converted to $<C_{10}$ products via fragmentation, C_{10} products via rearrangement (or H addition), or $>C_{10}$ products via recombination. C_{10} radical intermediates formed directly from *exo*-THDCP are more rapidly converted back to *exo*-THDCP in the presence of a more effective H donor and thereby the amounts of $<C_{10}$ and C_{10} demanded for producing $\geq C_{10}$ are more effectively reduced. The formation of $<C_{10}$ from C_{10} radical intermediates via fragmentation occurs independently of the H donor, although the H donor effects the formation of $<C_{10}$ from $<C_{10}$ radical intermediates. Thus, the formation of $<C_{10}$ ($\geq C_{10}$) is slowed but less (more) affected by a H donor. The formation of $<C_{10}$ ($\geq C_{10}$) can be less (more) effectively slowed in the presence of a more effective H donor. Consequently, the proposed mechanism in Figure 11 of ref 25 is consistent with the experimental results (i) and (ii) described above.

3.3. Thermal Decomposition Kinetics of *exo*-THDCP in the Presence of H donors. The kinetic analyses of the thermal decomposition of *exo*-THDCP in the absence and presence of THQ and THQox at 415 °C are shown in Figure 7. Generally, thermal decompositions of hydrocarbon fuels are assumed to be a first-order reaction in both the absence and presence of the H donor.[31,39] In the absence of the H donor, thermal decomposition of *exo*-THDCP studied here also showed first-order kinetics, because the plot of $\ln [RH]/[RH]_0$ versus reaction time t was a straight line (Figure 7a, black). This result is consistent with those reported previously.[10,20,23] In the presence of the H donor, however, the plot of $\ln [RH]/[RH]_0$ versus t was not a straight line. Thus, thermal decomposition of *exo*-THDCP cannot be a first-order reaction in the presence of the H donor. We therefore proposed the mechanism for the thermal decomposition of *exo*-THDCP in the presence of the H donor, whereby their thermal decomposition kinetics could be analyzed (see Section 2.2). Intriguingly, our experimental data for *exo*-THDCP and H donors at 395, 405, and 415 °C were well fitted to eqs 17 and 18 as shown in Figure 7a and b, respectively. Importantly, our kinetic mechanism explains the unusual thermal decomposition kinetics of *exo*-THDCP and H donors: (i) *exo*-THDCP does not follow first-order kinetics (Figure 7a, blue and red) and (ii) THQ and THQox show the S-shaped concentration−time curves (Figure 7b, blue and red).

The rate constants (k_1 and k_3) and k_4/k_2' at 395, 405, and 415 °C and the pre-exponential factor (k_0) and activation energy (E_a) for k_1 in the absence and presence of THQ and THQox are summarized in Table 2. Recall that k_1 and k_3 are the rate constants for the H abstraction of *exo*-THDCP and H donors, respectively. k_4/k_2' is the ratio of the rate constants for the two competing reactions, H addition to radical intermediates formed directly from *exo*-THDCP and their rearrangement (or fragmentation). That is, k_4/k_2' refers to the

dx.doi.org/10.1021/jp3113599 | J. Phys. Chem. C 2013, 117, 7399−7407

Table 2. Kinetic Data for the Thermal Decomposition of *exo*-THDCP in the Absence and Presence of THQ and THQox (0.5 wt %)[a]

					k_1	
H donor	temp (°C)	k_1 (s^{-1})	k_3 (s^{-1})	k_4/k_2' (M^{-1})	k_0 (s^{-1})	E_a (kJ/mol)
none	395	4.4×10^{-6}	–	–	5.0×10^{14}	256.4
	405	1.0×10^{-5}	–	–		
	415	1.7×10^{-5}	–	–		
THQ	395	8.0×10^{-7}	5.0×10^{-5}	7.2×10^{3}	7.0×10^{13}	254.5
	405	1.6×10^{-6}	5.1×10^{-5}	2.8×10^{3}		
	415	3.0×10^{-6}	5.1×10^{-5}	9.7×10^{2}		
THQox	395	4.0×10^{-8}	5.0×10^{-5}	1.5×10^{5}	3.5×10^{12}	252.6
	405	7.8×10^{-8}	5.0×10^{-5}	7.7×10^{4}		
	415	1.5×10^{-7}	5.1×10^{-5}	3.9×10^{4}		

[a]Kinetic parameters obtained from Figure 7. See details in Section 2.2.

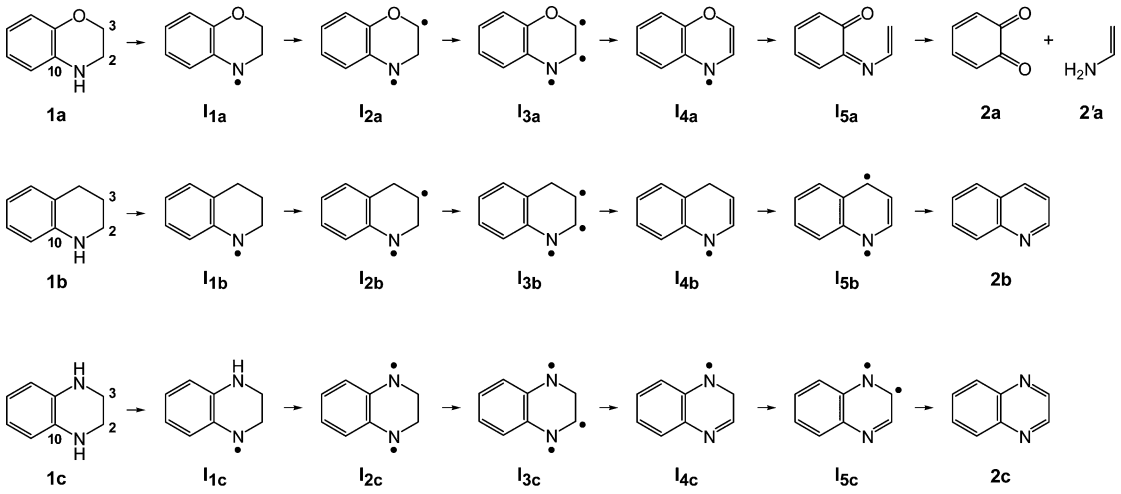

Figure 8. Proposed mechanism for H donations by Benzox, THQ, and THQox. H donors **1** undergo heterolytic cleavage to furnish hydrogen radicals, and concomitantly, intermediates **I** and products **2** are formed. See the detailed discussion in Section 3.4. For the relative energies and their diagrams, see Table 3 and Figure 9, respectively. Note that C2, C3, and C10 indicated here in Benzox are changed to C3, C2, and C4a, respectively, when the IUPAC system is used.

Table 3. Relative Energies of Intermediates and Products Formed from Benzox, THQ, and THQox upon H Donation[a]

	relative energy (kJ/mol)											
H donor	I_1		I_2		I_3		I_4		I_5		2	
Benzox	N1·	−18.7	C2·	−21.3	C2·	−28.8	N1=C10	21.3	N1=C10	−30.2	**2a** + **2'a**	−93.9
	C2·	−4.0	C3·	−25.9			C2=C3	−28.7				
	C3·	−6.9	N1=C10	21.3								
THQ	N1·	−19.9	C2·	−20.5	C2·	−17.6	C4·	−8.2	C4·	−8.2	C3=C4, N1=C2	−39.6
	C2·	−2.7	C3·	−35.0	C4·	−2.3	N1=C2	−33.6				
	C3·	−15.3	C4·	−11.8			C2=C3	−37.7				
	C4·	7.8	N1=C10	−19.9								
THQox	N1·	−19.8	C2·	−9.1	C2·	−28.4	N1=C2	−35.8	C3·	−26.9	C3=N4	−33.3
	C2·	11.5	C3·	−8.4	C3·	−28.4						
	C3·	11.5	N4·	−38.8								
	N4·	−19.8	N1=C10	−19.8								

[a]See details in Section 2.3. See also Figures 8 and 9. Xn is indicated in Figure 8.

effectiveness of H donors for lowering the thermal decomposition of *exo*-THDCP. In the absence and presence of THQ and THQox, k_1 increased with increasing temperature. The k_0 and E_a values for k_1 in the absence and presence of THQ and THQox were 5.0×10^{14} s^{-1} and 256.4 kJ/mol, 7.0×10^{13} s^{-1} and 254.5 kJ/mol, and 3.5×10^{12} s^{-1} and 252.6 kJ/mol, respectively. In the presence of THQ and THQox, k_4/k_2' decreased with increasing temperature, whereas k_3 remained nearly unchanged at 395−415 °C. k_1 for THQox was smaller than that for THQ. Thus, thermal decomposition of *exo*-THDCP via H abstraction (k_1) was slower in the presence of THQox compared to THQ. k_3 for THQox was nearly identical to that for THQ. Thus, consumptions of THQox and THQ via H abstraction (k_3) proceeded at similar rates. k_4/k_2' for THQox was greater than that for THQ. Thus, thermal decomposition of *exo*-THDCP via rearrangement or fragmentation (k_2') was

dx.doi.org/10.1021/jp3113599 | J. Phys. Chem. C 2013, 117, 7399−7407

more effectively counterbalanced via H addition (k_4) in the presence of THQox compared to THQ, which may be attributed to faster H donation by THQox relative to THQ. To investigate the differences in H-donation kinetics between THQox and THQ, we carried out molecular mechanics calculation.

3.4. Mechanisms for H Donations by Benzox, THQ, and THQox. The proposed mechanisms for H donations by Benzox, THQ, and THQox are shown in Figure 8 and Table 3. H donors **1** undergo heterolytic cleavage to furnish hydrogen radicals, and concomitantly, intermediates **I** and products **2** are formed. Benzox **1a** is fragmented to cyclohexa-3,5-diene-1,2-dione **2a** and ethenamine **2′a** via Claisen rearrangement of $\mathbf{I}_{5a}$. THQ **1b** and THQox **1c** are converted to quinoline **2b** and quinoxaline **2c**, respectively. **1a**, **1b**, and **1c** furnish hydrogen radicals from N1 and are then converted to $\mathbf{I}_{1a}$, $\mathbf{I}_{1b}$, and $\mathbf{I}_{1c}$, respectively. $\mathbf{I}_{1a}$ and $\mathbf{I}_{1b}$ furnish hydrogen radicals from C3 via Hofmann elimination-type heterolytic cleavage, whereas $\mathbf{I}_{1c}$ furnishes a hydrogen radical from N4.

The relative energy diagrams for H donations by Benzox, THQ, and THQox are shown in Figure 9. The energy of **2a** is

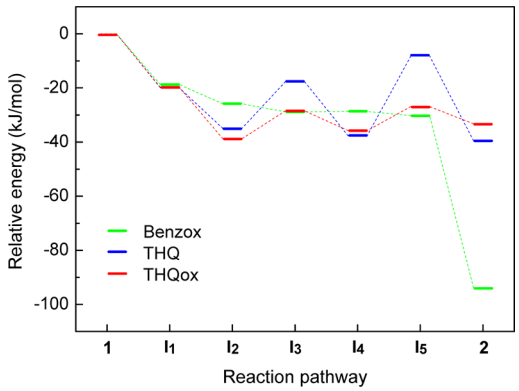

Figure 9. Relative energy diagrams for H donations by Benzox, THQ, and THQox. See details in Section 2.3. See also Figure 8 and Table 3. Note that the energy of **2a** + **2′a** (−93.9 kJ/mol) is not the sum of energies of **2a** (−48.8 kJ/mol) and **2′a** (−96.3 kJ/mol).

quite lower than those of **2b** and **2c**. Thus, **1a** can more rapidly furnish hydrogen radicals than **1b** and **1c**. However, **1a** appears to be fragmented to **2a** and **2′a** without furnishing hydrogen radicals. Thus, thermally unstable **1a** is incapable of furnishing hydrogen radicals. Accordingly, the thermal stability of *exo*-THDCP is hardly improved by Benzox. Overall, the energies of $\mathbf{I}_{1c}$−$\mathbf{I}_{5c}$ are lower than those of $\mathbf{I}_{1b}$−$\mathbf{I}_{5b}$. Thus, **1c** can more rapidly furnish hydrogen radicals than **1b**. Accordingly, THQox performs faster H donation than THQ and thereby the thermal stability of *exo*-THDCP is more effectively improved by THQox compared to THQ.

4. CONCLUSION

We investigated the thermal stability of *exo*-THDCP in the absence and presence of Benzox, THQ, and THQox, which act as H donors. The thermal stability of *exo*-THDCP was more effectively improved by THQox compared to THQ and Benzox. THQox was effective in improving the thermal stability of *exo*-THDCP even at high temperatures. We proposed the mechanism for the thermal decomposition of *exo*-THDCP in the presence of the H donor, whereby their unusual thermal decomposition kinetics could be analyzed. We also proposed the mechanism for H donations by Benzox, THQ, and THQox, whereby their distinct H-donation kinetics and thermal stability were elucidated and found to be associated with the more effective thermal stability improvement of *exo*-THDCP by THQox compared to THQ and Benzox.

■ ASSOCIATED CONTENT

Supporting Information

Figures and a table showing compositions of products and their comparison obtained upon thermal decomposition of *exo*-THDCP in the absence and presence of H donors. This material is available free of charge via the Internet at http://pubs.acs.org.

■ AUTHOR INFORMATION

Corresponding Author

*E-mail: kimsh@korea.ac.kr (S.H.K.); hogyuhan@korea.ac.kr (H.H.).

Author Contributions

‖These authors contributed equally to this work.

Notes

The authors declare no competing financial interest.

■ ACKNOWLEDGMENTS

This work was supported by the Korea University grant and the KETEP Human Resources Development (No. 2011-4010203050) grant to S.H.K.

■ REFERENCES

(1) Edwards, T. Liquid Fuels and Propellants for Aerospace Propulsion: 1903−2003. *J. Propul. Power* **2003**, *19*, 1089−1107.
(2) Edwards, T. Advancements in Gas Turbine Fuels from 1943 to 2005. *J. Eng. Gas Turbines Power* **2007**, *129*, 13−20.
(3) Burdette, G. W.; Lander, H. R.; McCoy, J. R. High-Energy Fuels for Cruise Missiles. *J. Energy* **1978**, *2*, 289−292.
(4) Chung, H. S.; Chen, C. S. H.; Kremer, R. A.; Boulton, J. R.; Burdette, G. W. Recent Developments in High-Energy Density Liquid Hydrocarbon Fuels. *Energy Fuels* **1999**, *13*, 641−649.
(5) Davidson, D. F.; Horning, D. C.; Herbon, J. T.; Hanson, R. K. Shock Tube Measurements of JP-10 Ignition. *Proc. Combust. Inst.* **2000**, *28*, 1687−1692.
(6) Li, S. C.; Varatharajan, B.; Williams, F. A. Chemistry of JP-10 Ignition. *AIAA J.* **2001**, *39*, 2351−2356.
(7) Wohlwend, K.; Maurice, L. Q.; Edwards, T.; Striebich, R. C.; Vangsness, M.; Hill, A. S. Thermal Stability of Energetic Hydrocarbon Fuels for Use in Combined Cycle Engines. *J. Propul. Power* **2001**, *17*, 1258−1262.
(8) Striebich, R. C.; Lawrence, J. Thermal Decomposition of High-Energy Density Materials at High Pressure and Temperature. *J. Anal. Appl. Pyrolysis* **2003**, *70*, 339−352.
(9) Osmont, A.; Gökalp, I.; Catoire, L. Evaluating Missile Fuels. *Propellants, Explos., Pyrotech.* **2006**, *31*, 343−354.
(10) Peela, N. R.; Kunzru, D. Thermal Cracking of JP-10: Kinetics and Product Distribution. *J. Anal. Appl. Pyrolysis* **2006**, *76*, 154−160.
(11) Nakra, S.; Green, R. J.; Anderson, S. L. Thermal Decomposition of JP-10 Studied by Micro-Flowtube Pyrolysis-Mass Spectrometry. *Combust. Flame* **2006**, *144*, 662−674.
(12) Herbinet, O.; Sirjean, B.; Bounaceur, R.; Fournet, R.; Battin-Leclerc, F.; Scacchi, G.; Marquaire, P.-M. Primary Mechanism of the Thermal Decomposition of Tricyclodecane. *J. Phys. Chem. A* **2006**, *110*, 11298−11314.
(13) Parsinejad, F.; Arcari, C.; Metghalchi, H. Flame Structure and Burning Speed of JP-10 Air Mixtures. *Combust. Sci. Technol.* **2006**, *178*, 975−1000.

(14) Van Devener, B.; Anderson, S. L. Breakdown and Combustion of JP-10 Fuel Catalyzed by Nanoparticulate CeO_2 and Fe_2O_3. *Energy Fuels* **2006**, *20*, 1886−1894.
(15) Han, K.-J.; Hwang, I.-C.; Park, S.-J.; Choi, M.-J.; Lee, S.-B.; Han, J.-S. Vapor−Liquid Equilibrium, Densities and Viscosities for the Binary System *exo*- and *endo*-Tetrahydrodicyclopentadiene and Pure Component Vapor Pressures. *Fluid Phase Equilib.* **2006**, *249*, 187−191.
(16) Li, D.; Fang, W.; Xing, Y.; Guo, Y.; Lin, R. Spectroscopic Studies on Thermal-Oxidation Stability of Hydrocarbon Fuels. *Fuel* **2008**, *87*, 3286−3291.
(17) Xing, Y.; Fang, W.; Xie, W.; Guo, Y.; Lin, R. Thermal Cracking of JP-10 under Pressure. *Ind. Eng. Chem. Res.* **2008**, *47*, 10034−10040.
(18) Xie, W.; Fang, W.; Li, D.; Xing, Y.; Guo, Y.; Lin, R. Coking of Model Hydrocarbon Fuels under Supercritical Condition. *Energy Fuels* **2009**, *23*, 2997−3001.
(19) Jiao, C. Q.; Ganguly, B. N.; Garscadden, A. Mass Spectrometry Study of Decomposition of *exo*-Tetrahydrodicyclopentadiene by Low-Power, Low-Pressure rf Plasma. *J. Appl. Phys.* **2009**, *105*, 033305.
(20) Chenoweth, K.; van Duin, A. C. T.; Dasgupta, S.; Goddard, W. A., III. Initiation Mechanisms and Kinetics of Pyrolysis and Combustion of JP-10 Hydrocarbon Jet Fuel. *J. Phys. Chem. A* **2009**, *113*, 1740−1746.
(21) Hudzik, J. M.; Asatryan, R.; Bozzelli, J. W. Thermochemical Properties of *exo*-Tricyclo[5.2.1.$0^{2,6}$]decane (JP-10 Jet Fuel) and Derived Tricyclodecyl Radicals. *J. Phys. Chem. A* **2010**, *114*, 9545−9553.
(22) Seiser, R.; Niemann, U.; Seshadri, K. Experimental Study of Combustion of *n*-Decane and JP-10 in Non-premixed Flows. *Proc. Combust. Inst.* **2011**, *33*, 1045−1052.
(23) Magoon, G. R.; Aguilera-Iparraguirre, J.; Green, W. H.; Lutz, J. J.; Piecuch, P.; Wong, H.-W.; Oluwole, O. O. Detailed Chemical Kinetic Modeling of JP-10 (*exo*-Tetrahydrodicyclopentadiene) High-Temperature Oxidation: Exploring the Role of Biradical Species in Initial Decomposition Steps. *Int. J. Chem. Kinet.* **2012**, *44*, 179−193.
(24) Park, S. H.; Kwon, C. H.; Kim, J.; Chun, B.-H.; Kang, J. W.; Han, J. S.; Jeong, B. H.; Kim, S. H. Thermal Stability and Isomerization Mechanism of *exo*-Tetrahydrodicyclopentadiene: Experimental Study and Molecular Modeling. *Ind. Eng. Chem. Res.* **2010**, *49*, 8319−8324.
(25) Park, S. H.; Kim, J.; Chun, J. H.; Chung, W.; Lee, C. H.; Chun, B.-H.; Han, J. S.; Jeong, B. H.; Han, H.; Kim, S. H. Mechanistic Insights into Thermal Stability Improvement of *exo*-Tetrahydrodicyclopentadiene by 1,2,3,4-Tetrahydroquinoline. *Ind. Eng. Chem. Res.* **2012**, *51*, 14949−14957.
(26) Park, S. H.; Kim, J.; Chun, J. H.; Chung, W.; Kim, S. G.; Lee, C. H.; Chun, B.-H.; Han, J. S.; Jeong, B. H.; Han, H.; Kim, S. H. Metal Effects on the Thermal Decomposition of *exo*-Tetrahydrodicyclopentadiene. *Ind. Eng. Chem. Res.* **2013**, *52*, 4395−4400.
(27) Coleman, M. M.; Selvaraj, L.; Sobkowiak, M.; Yoon, E. Potential Stabilizers for Jet Fuels Subjected to Thermal Stress above 400 °C. *Energy Fuels* **1992**, *6*, 535−539.
(28) Selvaraj, L.; Sobkowiak, M.; Song, C.; Stallman, J. B.; Coleman, M. M. A Model System for the Study of Additives Designed to Enhance the Stability of Jet Fuels at Temperatures above 400 °C. *Energy Fuels* **1994**, *8*, 839−845.
(29) Song, C.; Lai, W.-C.; Schobert, H. H. Hydrogen-Transferring Pyrolysis of Long-Chain Alkanes and Thermal Stability Improvement of Jet Fuels by Hydrogen Donors. *Ind. Eng. Chem. Res.* **1994**, *33*, 548−557.
(30) Yoon, E. M.; Selvaraj, L.; Song, C.; Stallman, J. B.; Coleman, M. M. High-Temperature Stabilizers for Jet Fuels and Similar Hydrocarbon Mixtures. 1. Comparative Studies of Hydrogen Donors. *Energy Fuels* **1996**, *10*, 806−811.
(31) Yoon, E. M.; Selvaraj, L.; Eser, S.; Coleman, M. M. High-Temperature Stabilizers for Jet Fuels and Similar Hydrocarbon Mixtures. 2. Kinetic Studies. *Energy Fuels* **1996**, *10*, 812−815.
(32) Beaver, B. D.; Gao, L.; Fedak, M. G.; Coleman, M. M.; Sobkowiak, M. Model Studies Examining the Use of Dicyclohexylphenylphosphine to Enhance the Oxidative and Thermal Stability of Future Jet Fuels. *Energy Fuels* **2002**, *16*, 1134−1140.
(33) Beaver, B. D.; Burgess Clifford, C.; Fedak, M. G.; Gao, L.; Iyer, P. S.; Sobkowiak, M. High Heat Sink Jet Fuels. Part 1. Development of Potential Oxidative and Pyrolytic Additives for JP-8. *Energy Fuels* **2006**, *20*, 1639−1646.
(34) Sobkowiak, M.; Burgess Clifford, C.; Beaver, B. High Heat Sink Jet Fuels. 2. Stabilization of a JP-8 with Model Refined Chemical Oil/Light Cycle Oil (RCO/LCO)-Derived Stabilizers. *Energy Fuels* **2007**, *21*, 982−986.
(35) Beaver, B.; Sobkowiak, M.; Burgess Clifford, C.; Wei, Y.; Fedek, M. High Heat Sink Jet Fuels. 3. On the Mechanisms of Action of Model Refined Chemical Oil/Light Cycle Oil (RCO/LCO)-Derived Stabilizers for JP-8. *Energy Fuels* **2007**, *21*, 987−991.
(36) Liu, G.; Han, Y.; Wang, L.; Zhang, X.; Mi, Z. Solid Deposits from Thermal Stressing of *n*-Dodecane and Chinese RP-3 Jet Fuel in the Presence of Several Initiators. *Energy Fuels* **2009**, *23*, 356−365.
(37) Guo, W.; Zhang, X.; Liu, G.; Wang, J.; Zhao, J.; Mi, Z. Roles of Hydrogen Donors and Organic Selenides in Inhibiting Solid Deposits from Thermal Stressing of *n*-Dodecane and Chinese RP-3 Jet Fuel. *Ind. Eng. Chem. Res.* **2009**, *48*, 8320−8327.
(38) Bruno, T. J.; Wolk, A.; Naydich, A. Stabilization of Biodiesel Fuel at Elevated Temperature with Hydrogen Donors: Evaluation with the Advanced Distillation Curve Method. *Energy Fuels* **2009**, *23*, 1015−1023.
(39) Widegren, J. A.; Bruno, T. J. Thermal Decomposition Kinetics of Kerosene-Based Rocket Propellants. 1. Comparison of RP-1 and RP-2. *Energy Fuels* **2009**, *23*, 5517−5522.
(40) Widegren, J. A.; Bruno, T. J. Thermal Decomposition Kinetics of Kerosene-Based Rocket Propellants. 2. RP-2 with Three Additives. *Energy Fuels* **2009**, *23*, 5523−5528.
(41) Widegren, J. A.; Bruno, T. J. Thermal Decomposition Kinetics of Kerosene-Based Rocket Propellants. 3. RP-2 with Varying Concentrations of the Stabilizing Additive 1,2,3,4-Tetrahydroquinoline. *Energy Fuels* **2011**, *25*, 288−292.
(42) MacDonald, M. E.; Davidson, D. F.; Hanson, R. K. Decomposition Measurements of RP-1, RP-2, JP-7, *n*-Dodecane, and Tetrahydroquinoline in Shock Tubes. *J. Propul. Power* **2011**, *27*, 981−989.
(43) Kim, J.; Park, S. H.; Lee, C. H.; Chun, B.-H.; Han, J. S.; Jeong, B. H.; Kim, S. H. Coke Formation during Thermal Decomposition of Methylcyclohexane by Alkyl Substituted C_5 Ring Hydrocarbons under Supercritical Conditions. *Energy Fuels* **2012**, *26*, 5121−5134.
(44) Allinger, N. L.; Yuh, Y. H.; Lii, J.-H. Molecular Mechanics. The MM3 Force Field for Hydrocarbons. 1. *J. Am. Chem. Soc.* **1989**, *111*, 8551−8566.
(45) Lii, J.-H.; Allinger, N. L. Molecular Mechanics. The MM3 Force Field for Hydrocarbons. 3. The van der Waals' Potentials and Crystal Data for Aliphatic and Aromatic Hydrocarbons. *J. Am. Chem. Soc.* **1989**, *111*, 8576−8582.
(46) Langley, C. H.; Lii, J.-H.; Allinger, N. L. Molecular Mechanics Calculations on Carbonyl Compounds. IV. Heats of Formation. *J. Comput. Chem.* **2001**, *22*, 1476−1483.